MOLECULAR AND CELLULAR BIOLOGY, Oct. 2005, p. 8874–8886 Vol. 25, No. 20
0270-7306/05/$08.00+0 doi:10.1128/MCB.25.20.8874–8886.2005

Nucleophosmin Is Required for DNA Integrity and p19^{Arf} Protein Stability†

Emanuela Colombo,[1] Paola Bonetti,[1] Eros Lazzerini Denchi,[1,2]‡ Paola Martinelli,[1] Raffaella Zamponi,[1] Jean-Christophe Marine,[3] Kristian Helin,[1] Brunangelo Falini,[4] and Pier Giuseppe Pelicci[1,2,5]*

Department of Experimental Oncology, European Institute of Oncology, Via Ripamonti 435, 20141 Milan, Italy[1]; IFOM Institute, Via Adamello 16, 20139 Milan, Italy[2]; Laboratory for Molecular Cancer Biology, Flanders Interuniversity Institute for Biotechnology, University of Ghent, B-9052 Ghent, Belgium[3]; Institute of Hematology and Internal Medicine, University of Perugia, 06100 Perugia, Italy[4]; and Department of Medicine, Surgery and Dentistry, University of Milan, Milan, Italy[5]

Received 24 June 2005/Returned for modification 2 July 2005/Accepted 21 July 2005

Nucleophosmin (NPM) is a nucleolar phosphoprotein that binds the tumor suppressors p53 and p19^{Arf} and is thought to be indispensable for ribogenesis, cell proliferation, and survival after DNA damage. The NPM gene is the most frequent target of genetic alterations in leukemias and lymphomas, though its role in tumorigenesis is unknown. We report here the first characterization of a mouse NPM knockout strain. Lack of NPM expression results in accumulation of DNA damage, activation of p53, widespread apoptosis, and mid-stage embryonic lethality. Fibroblasts explanted from null embryos fail to grow and rapidly acquire a senescent phenotype. Transfer of the NPM mutation into a p53-null background rescued apoptosis in vivo and fibroblast proliferation in vitro. Cells null for both p53 and NPM grow faster than control cells and are more susceptible to transformation by activated oncogenes, such as mutated Ras or overexpressed Myc. In the absence of NPM, Arf protein is excluded from nucleoli and is markedly less stable. Our data demonstrate that NPM regulates DNA integrity and, through Arf, inhibits cell proliferation and are consistent with a putative tumor-suppressive function of NPM.

Nucleophosmin (NPM; also known as B23, NO38, or numatrin) is an abundant and ubiquitously expressed nucleolar phosphoprotein which has been implicated in ribosome biogenesis (41). Indeed, NPM binds nucleic acids (11), associates with maturing preribosomal ribonucleoprotein particles (27), and possesses intrinsic RNase activity (33) and its down-regulation retards the processing of pre-rRNA (18). NPM acts as a molecular chaperone (36) and shuttles between the nucleus and cytoplasm (3), suggesting that it may also prevent aggregation of nucleolar proteins and facilitate nuclear export.

NPM has the additional property of regulating cell proliferation, though its specific effect remains controversial. Down-regulation of NPM in normal or immortalized cells delays cell division (6) or induces apoptosis (18), while its overexpression induces growth arrest in normal cells (9, 18) and stimulates S-phase entry in immortalized cells (18). The level of NPM protein increases when cells are induced to proliferate (15) and decreases when they differentiate (17).

NPM has also been implicated in the acute response of mammalian cells to environmental stresses, particularly DNA-damaging agents. UV light, for example, induces up-regulation (39) and nuclear relocalization of NPM (22) that, under these experimental conditions, stimulates DNA repair and reduces apoptosis (40).

NPM is part of a high-molecular-weight complex and physically interacts with many cellular proteins, including p53 (9), Mdm2 (22), and Arf (2, 18, 20). p53 is a tumor suppressor that is mutated in more than 50% of human cancers and accumulates in response to DNA damage and oncogene activation (16). When stabilized and activated, p53 initiates a transcriptional program that leads to either cell cycle arrest or apoptosis (37). The stability of the p53 protein is primarily regulated by Mdm2, a ubiquitin E3 ligase, and Arf (p19^{Arf} in the mouse and p14^{Arf} in humans), a nucleolar protein that binds p53 and antagonizes Mdm2's ubiquitin ligase activity for p53 (32). Despite several reports, it remains unclear whether interactions of NPM with p53, Mdm2, and Arf underlie the effects of NPM on ribogenesis, cellular growth, and survival.

NPM increases the stability and transcriptional activity of p53, likely through multiple mechanisms, including its chaperone activity on p53, inhibition of the Mdm2 ubiquitin-ligase activity, and competition with p53-Mdm2 binding (9, 22). Other laboratories, however, using different cell systems and experimental approaches, have reported an inhibitory effect of NPM on phosphorylation of p53 and attenuation of its transcriptional effects (23).

The Arf-NPM interaction seems to be critical in regulating the stability of both proteins. Arf, in fact, induces polyubiquitination and degradation of NPM and inhibits its effects on ribogenesis (18). NPM, instead, protects Arf from degradation

* Corresponding author. Mailing address: European Institute of Oncology, Via Ripamonti 435, 20141 Milan, Italy. Phone: 39-02-57489838. Fax: 39-02-57489851. E-mail: piergiuseppe.pelicci@ifom-ieo-campus.it.

† Supplemental material for this article may be found at http://mcb.asm.org/.

‡ Present address: The Rockefeller University, 1230 York Avenue, New York, N.Y.

and, surprisingly, antagonizes its ability to inhibit cell division (20).

The effects of NPM on the Arf-Mdm2-p53 tumor suppressor pathway, as well as its activities on ribogenesis, cell division, and survival, might be relevant for the role of NPM in human cancer. NPM, in fact, is frequently overexpressed in tumors of different origin (8, 25) and is the most frequent target of genetic alterations in hematopoietic tumors: it is rearranged with the ALK gene in the majority of anaplastic large-cell lymphomas (24) and is mutated in 35% of acute myeloid leukemias (13). The biological contribution of NPM mutant alleles to transformation and the underlying molecular mechanisms remain, however, undetermined.

To investigate the physiological function of NPM we have generated and analyzed a mouse line null for the expression of NPM. Our investigations shed a new light on the genetic and functional interactions of NPM with p53 and Arf and provide the first interpretation of the biological activity of cancer-associated NPM mutants.

MATERIALS AND METHODS

Generation of NPM-deficient mice. NPM-deficient mice were generated by Lexicon Genetics Inc. (The Woodlands, TX). An embryonic stem (ES) cell clone with a single gene trap event in the *NPM* locus was used to generate the *NPM*-deficient mouse line (genetic background: C57BL/6 × 129/Ola) (43). The vector used to create this particular ES cell clone was VICTR37 (8.1 kb) containing a splicing acceptor site, an internal ribosome entry site-BGeo cassette for positive selection, and the splice donor site of the first exon of the *BTK* gene. The insertion was determined by genomic PCR and occurred 488 bp downstream of exon I (AACCTACAGGTGGGGTCTTTCA*GTCCGAGCAGGCGCCCTGAGG; the retroviral long terminal repeat sequence is underlined, and the asterisk indicates the insertion site).

PCR genotyping. A PCR-based strategy was developed to distinguish wild-type and mutant NPM alleles. The following primers were used: 5′-TAGAAGCAG CGGCCTGAACACTA; 5′GATGCTGACTCCGCCTACCAGA; and 5′-GCCT TGCAAAATGGCGTTACTT (see Fig. 1A). A 336-bp fragment indicates the presence of the mutated allele, whereas a 641-bp fragment is amplified from the wild-type allele (see Fig. 1B). Trp53 genotyping was determined as previously described (19)

Histology. For sectioning, embryos were fixed in 4% paraformaldehyde 1-phosphate-buffered saline overnight, embedded in paraffin, sectioned, and stained in hematoxylin and eosin.

Immunohistochemistry. For bromodeoxyuridine (BrdU) experiments, pregnant females were injected intraperitoneally with 150 μg of BrdU/g of body weight and sacrificed 2 h later. The following antisera were used: anti-BrdU (1/200; Boehringer Mannheim), anti-cleaved caspase 3 (1/200; Cell Signaling), anti-NPM (NPMc) (10), anti-H2AX (1:100; Upstate), and anti-p53 (monoclonal antibody raised against mouse p53 protein, clone AI25, kindly provided by Kristian Helin) An appropriate biotinylated secondary antibody was then applied to the slides. Avidin-conjugated peroxidase (ABC and DAB kits from Vector Laboratories) was used for immunostaining.

TaqMan real-time quantitative reverse transcription-PCR assays. Total RNA (1 μg) was reverse transcribed in a final volume of 20 ul using a commercial kit (Gibco-BRL). The quantitative PCR assays were performed following the manufacturer's specifications (PE Applied Biosystems). Primer pairs and TaqMan probes were designed by Applied Biosystems. Each sample was analyzed in triplicate.

Immunoblotting and immunoprecipitation. Western blot experiments were performed as described (9). The primary antibodies used were: sheep polyclonal anti-p53 (1:1000; Ab7; Oncogene); rabbit polyclonal anti-p53 phospho-Ser15 (1/1,000; Cell Signaling), monoclonal anti-p21 (1/300; F5; Santa Cruz); polyclonal anti-p19^{Arf} (1:1,000; Abcam); monoclonal anti-NPM (NPMc; NPMa) (10); polyclonal anti-β-tubulin (1:1,000, H-235, Santa Cruz); monoclonal antivinculin (1:1,000; hVIN-1; Sigma), monoclonal anti-Flag (1:1,000; Sigma), polyclonal anti-NPM (B19) (9), and anti-H2AX (1:1,000; Upstate)

Immunofluorescence. Immunofluorescence analysis was performed as previously described (9). The antibodies used were polyclonal anti-p19^{Arf} (1:200; Abcam); monoclonal anti-NPM (NPMc), monoclonal antinucleolin (1:500; MS-3; Santa Cruz); polyclonal antifibrillarin (1:300; A-16; Santa Cruz), antiphosphorylated ATM (1:500; Rockland), and anti-γH2AX (1:300; Upstate).

Cell culture, transfection, and infection. Mouse embryo fibroblasts (MEFs), Phoenix, and 293T cells were cultured at 37°C and 5% CO_2 in Dulbecco's modified Eagle's medium supplemented with 10% fetal bovine serum. Transient transfections were performed using the standard calcium phosphate precipitate method for Phoenix and 293T cells and FuGENE 6 (Roche) for MEFs. For infection experiments, we used a Pinco-based vector expressing either only the green fluorescent protein (GFP) or GFP-tagged wild-type NPM and mutant protein. For expression of RasV12, c-*myc*, and p19^{Arf} we used the pBabe retroviral vector carrying puromycin resistance. For interference experiments we used a lentivirus-based vector called Lentilox3.7 (31). Empty or recombinant retroviral or lentivirus vectors were transfected into the Phoenix and 293T packaging cell lines, respectively, and after 48 h the supernatants were used to infect target cells.

Cell cycle analysis. Replicative DNA synthesis and DNA content were analyzed using bivariate flow cytometry. Experiments have been carried out as described previously (9). Briefly, cells were pulsed with BrdU 1 μM, fixed and treated with 2 M HCl for 20 min followed by 2 volumes of 0.1 M sodium borate (pH 8.5). After washing cells were incubated with anti-BrdU antibody for 1 hour, washed and incubated with fluorescein isothiocyanate-conjugated secondary antibody. Cells were counterstaining overnight with 5 μg/ml propidium iodide.

Plasmids. For short interfering RNA we used a lentivirus-based vector (Lentilox 3.7), in which we cloned (HpaI-XhoI cloning sites) the following double-stranded oligonucleotides. For NPM interference we used two different double-standard oligonucleotides that targeted two different regions of NPM mRNA (for region 1, FW 5′TggctgacaaagactatcacTTCAAGAGAgtgatagtctttgtcagccTT TTTTC and REV 5′TCGAGAAAAAAggctgacaaagactatcacTCTCTTGAAgtgat agtctttgtcagccA; for region 2, FW 5′TgagcaccagttgtcattaaTTCCAAGAGAttaa tgacaactggtgcAcTTTTTTC and REV 5′TCGAGAAAAAAgagcaccagttgtcattaa TCTCTTGGAAttaatgacaactggtgcAcA). Lowercase letters represent the region that matches with the sequence of the targeted gene, and uppercase letters represent the common part of the oligonucleotides required for cloning and hairpin formation.

Analysis of newly synthesized rRNA. Experiments have been performed as previously described (2). Briefly, cells were labeled with 2.5 uCi of [^{3}H]uridine per ml in complete medium for 30 min, washed twice, and then incubated in complete medium without the radioactive precursor for 2 h. Total RNA was isolated with Trizol (Invitrogen), quantitated, and loaded into 1% agarose gels containing formaldehyde. After electrophoretic separation the RNA was transferred to Hybond N$^+$ membranes (Amersham), and dried membranes were treated with En^{3}Hance (Perkin Elmer) and then subjected to autoradiography.

Yolk sac cell preparation. The yolk sac was dissected from 10.5-day embryos, rinsed to remove maternal blood, and incubated with 0,1% collagenase (Sigma) in 20% fetal bovine serum for 45 min at 37°C. Dispersed yolk sac was drawn through a 70-um strainer and washed with Iscove's minimal medium plus 10% fetal bovine serum. The cell suspension was counted and seeded in semisolid medium 3236 (StemCell Technologies) supplemented with 15% fetal bovine serum, 100 ng/ml stem cell factor, 5 ng/ml interleukin-3 and interleukin-6. After 10 days colonies can be counted and collected cells are replated. After the first replating the cell population have been cultured both in semisolid or liquid (Dulbecco's modified Eagle's medium) medium.

RESULTS

Mid-stage embryonic lethality of NPM$^{-/-}$ embryos. An ES cell clone with a specific gene trap event in the NPM locus was microinjected into host blastocysts to produce an NPM gene trap mouse line (43). The insertion gene trap vector, based on Moloney murine leukemia virus, integrated between exon 1 and exon 2 of the NPM locus (Fig. 1A). Mice heterozygous for this mutation were viable and fertile. However, matings between heterozygous animals produced no viable homozygous mutant offspring (F_2 in Table 1), indicating a recessive lethal phenotype (see Fig. 1B for representative genotypes and Western blots of wild-type and mutated NPM tissues).

Closer inspection revealed that all homozygous embryos (NPM$^{-/-}$) died in utero between 9.5 and 10.5 days postcoitum (dpc) (Table 1) and exhibited marked growth deficiency and

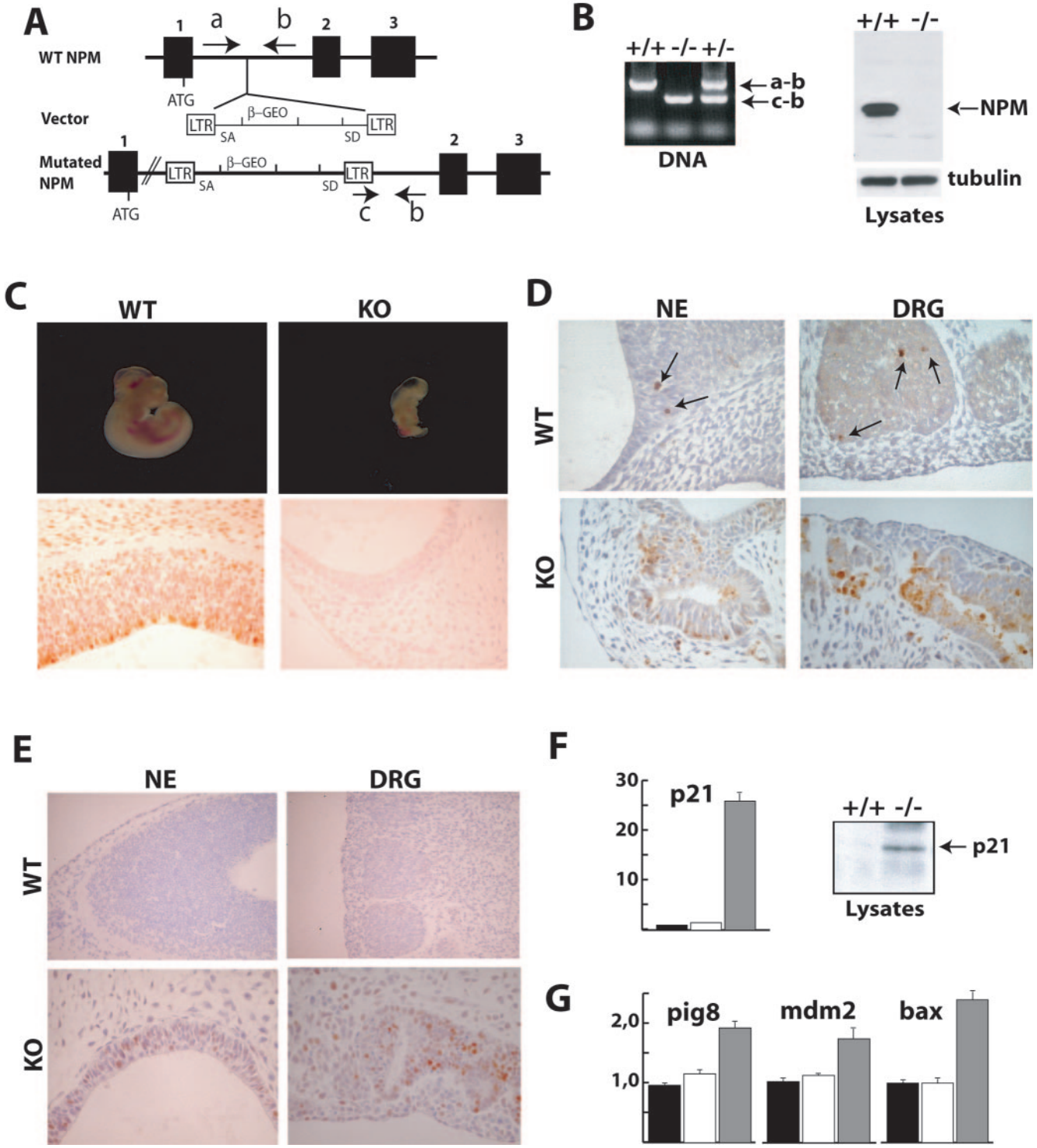

FIG. 1. Gene trap event in the NPM locus leads to a null NPM mutation and early embryonic lethality in mice. (A) Schematic representation of the targeting retroviral construct (middle) and the wild-type (upper) or mutated (lower) NPM alleles. Positions of oligonucleotides used for the PCR-based genotyping (see panel B) are indicated by arrows (a, b, and c). LTR: long terminal repeats; SA: splicing acceptor site; SD: splicing donor sites; β-Geo: neomycin resistance gene. (B) Left panel: PCR analysis of embryos with the indicated NPM genotypes (primer pairs used are indicated on the right). Right panel: expression of NPM protein as determined by Western blotting of lysates prepared from whole embryos. A polyclonal antibody anti-NPM (Santa Cruz) was used. (C) Wild-type (WT) and knockout (KO) NPM embryos at 10.5 dpc of embryonic development (upper panels) and immunohistochemistry analysis of NPM expression in neuroepithelial (NE) sections from the same embryos, using NPMc antibodies (lower panels). (D and E) immunohistochemistry analysis of apoptosis (D; anti-caspase-3 staining) and p53 expression levels (E; anti-p53 staining) in the developing neuroepithelium and dorsal root ganglia (DRG) of wild-type NPM and knockout 10.5 dpc embryos. (F and G) Expression of p53 target genes analyzed by quantitative PCR (*p21*, *Pig8*, *Mdm2*, and *Bax*) using mRNA from wild-type NPM (black bars), heterozygous (white bars), and knockout (gray bars) embryos. (G) Western blotting analysis of p21 protein expression in total embryo lysates.

TABLE 1. Genotype analysis of progeny from NPM heterozygous intercrosses

Stage	No. of litters	Total no. of embryos	No. of embryos with NPM genotype:			No. of abnormal embryos[a]	NPM$^{-/-}$ (%)[b]
			+/+	+/−	−/−		
E9.5	1	12	4	6	2	2	17
E10.5	6	55	15	27	13	13	24
E11.5	2	16	7	9	0	0	0
E12.5	2	14	6	8	0	1	0
F_2	30	142	54	88	0		

[a] Number of embryos with a growth defect and/or gross abnormalities.
[b] Percentage of embryos with NPM$^{-/-}$ genotype.

gross developmental alterations (Fig. 1C). Histological examination of various embryonic tissues from NPM$^{-/-}$ mutants did not reveal developmental features characteristic of their embryonic stage, suggesting that the growth defect is due to a developmental arrest (Fig. 1C, representative sections of neuroepithelium from wild-type and null 10.5 dpc embryos; see also Fig. S1 in the supplemental material). No viable mutants were observed beyond embryonic day E10.5 (Table 1). Consistent with an overall impact of the mutation throughout the whole embryo at 9.5 to 10.5 dpc, NPM was highly and ubiquitously expressed at this developmental stage, as demonstrated by immunohistochemistry (Fig. 1C). The placental structures of NPM$^{-/-}$ embryos were smaller but normally developed (not shown).

p53-dependent apoptosis in the NPM$^{-/-}$ embryos. To investigate the cellular basis of the embryonic lethality associated with the NPM mutation, we investigated the effect of NPM expression on apoptosis by measuring in situ activation of caspase-3 by immunohistochemistry. Caspase-3-positive cells were only occasionally observed in wild-type embryos, as expected. In the mutant embryos, instead, caspase-3-positive cells were present at a high proportion in all the tissues examined (Fig. 1D for representative results). To investigate the molecular basis for the increased apoptosis in the NPM-null embryos, we measured levels of p53 expression by immunohistochemistry. Anti-p53 staining was low or undetectable in the wild-type embryos, while a large number of p53-positive cells were found in all NPM$^{-/-}$ embryonic tissues (Fig. 1E for representative results). Quantitative PCR and Western blotting analysis of a number of p53 target genes (*p21*, *Mdm2*, *pig8*, and *Bax*) confirmed the transcriptional competence of stabilized p53 in the knockout embryo (Fig. 1F and G). It appears, therefore, that p53 is constitutively activated in NPM$^{-/-}$ embryonic cells.

To investigate whether p53 activation is responsible for the observed mid-stage embryonic lethality, widespread embryo apoptosis, and in vitro MEF senescence, the NPM mutation was transferred into a p53-null background (19). Matings between NPM$^{+/-}$ and p53$^{+/-}$ or p53$^{-/-}$ mice produced no viable doubly homozygous mutant offspring, indicating that the absence of p53 does not rescue embryonic lethality of the NPM mutation (Table 2). Analysis of embryo development revealed the presence of double-knockout embryos up to 12.5 dpc, a stage when all NPM$^{-/-}$ embryos have been readsorbed (Table 3). Moreover, the NPM$^{-/-}$ p53$^{-/-}$ (double-knockout) embryos were bigger and more developed than NPM$^{-/-}$ embryos at the same developmental stage and more similar to their p53$^{-/-}$ controls (compare Fig. 2A with Fig. 1C). Analysis of anti-caspase-3-positive cells revealed a marked reduction of apoptotic cells in the double-knockout mutant compared to NPM$^{-/-}$ embryos (Fig. 2B). It appears, therefore, that loss of p53 has a moderate effect on the mid-stage embryonic lethality associated with mutation of NPM, while it rescues the apoptosis observed in vivo.

NPM$^{-/-}$ cells can be grown in vitro only if p53 is lost (double-knockout MEFS) or functionally inhibited (yolk sac cells). We then tried to propagate in vitro fibroblasts from NPM$^{-/-}$ and wild-type embryos (MEFs). Upon seeding, the fibroblasts adhered to the culture dishes, did not proliferate, and acquired a senescence-like phenotype (not shown). This experiment was performed several times using MEF preparations from NPM$^{-/-}$ embryos at different stages (9, 10, and 10.5 dpc), and always gave the same result.

To investigate whether the growth arrest observed in NPM$^{-/-}$ MEFs is the direct consequence of NPM deficiency, we down-regulated expression of NPM in growing wild-type MEFs using lentivirus vectors expressing NPM-specific short hairpin RNAs (siNPM). Expression of siNPM led to the almost complete disappearance of the NPM protein in about 70% of the infected cells, as evaluated by immunofluorescence analysis (Fig. 2C). Western blot analysis of the same cell population revealed a consistent decrease in cell proliferation of fibroblast infected with the siNPM lentivirus (Fig. 2C). Analysis of BrdU incorporation performed in the same experiment (day 3) showed a dramatic decrease of BrdU-positive cells in the MEFs infected with the siNPM lentivirus compared to control cultures (from 27 to7% in the experiment shown in Fig. 2C). Comparable results were obtained using lentivirus vectors that expressed different NPM-specific short hairpin RNAs (not shown; see Materials and Methods). It appears, therefore, that

TABLE 2. Genotypes of mice from NPM$^{+/-}$ p53$^{+/-}$ × NPM$^{+/-}$ p53$^{+/-}$ crosses

Genotype	No. of mice			Total no. of mice
	NPM$^{+/+}$	NPM$^{+/-}$	NPM$^{-/-}$	
p53$^{+/+}$	13	44	0	57
p53$^{+/-}$	24	60	0	84
p53$^{-/-}$	25	26	0	51
Total	62	130	0	192

TABLE 3. Genotype analysis of progeny from $NPM^{+/-}$ $p53^{-/-}$ × $NPM^{+/-}$ $p53^{+/+}$ intercrosses

Stage	No. of litters	Total no. of embryos	No. of embryos with NPM genotype:			No. of abnormal embryos[a]	$NPM^{-/-}$ (%)[b]
			+/+	+/−	−/−		
E10.5	2	16	2	10	4	4	25
E11.5	2	33	8	20	5	5	15
E12.5	2	15	4	10	1	1	6

[a] Number of embryos with a growth defect and/or gross abnormalities.
[b] Percentage of embryos with $NPM^{-/-}$ genotype.

depletion of NPM expression in wild-type MEFs induces cell cycle arrest, suggesting that the growth arrest observed with $NPM^{-/-}$ MEFs is a cell-autonomous effect due to NPM deficiency.

Notably, wild-type MEFs infected with siNPM lentiviruses expressed moderately higher protein levels of the p53 target p21 compared to control cultures (Fig. 2C), suggesting that the cell cycle arrest observed after NPM depletion is due to p53 activation. This hypothesis was confirmed by the finding that MEFs derived from double-knockout embryos did not undergo growth arrest in culture and showed unlimited growth potential (as evaluated by the 3T3 assay; not shown). The growth properties of double-knockout MEFs are described below (Fig. 4B).

Activation of p53 is antagonized by cytokines, as shown by the finding that hematopoietic precursors grown in vitro in the presence of cytokines are resistant to p53-induced apoptosis (30). Therefore, we investigated whether $NPM^{-/-}$ hematopoietic cells can be propagated in vitro. Single-cell suspensions from E9.5 to E10.5 yolk sacs were plated in methylcellulose in the presence of cytokines and macroscopic colonies (CFC) were scored after 14 days. Thereafter, single-cell suspensions from pooled primary CFC colonies were replated into secondary CFC cultures or grown in liquid cultures.

As we had hypothesized, $NPM^{-/-}$ yolk sac cells were able to grow under both culture conditions (Fig. 2D, left panel, and data not shown). On the contrary, 24 h of cytokine deprivation provoked a marked reduction of the ability of $NPM^{-/-}$ cells to form CFCs, while had no effect on wild-type cells (Fig. 2D, right panel). Reexpression of NPM in cytokine-deprived $NPM^{-/-}$ cells restored the normal levels of CFC colonies (Fig. 2D). It appears, therefore, that $NPM^{-/-}$ yolk sac cells can be propagated in vitro only if grown in the presence of cytokines.

Analysis of the number of CFC colonies, however, showed that the efficiency of colony formation and growth rate of $NPM^{-/-}$ yolk sac cells (in the presence of cytokines) was slightly, yet consistently, lower than that of control wild-type cells (Fig. 2D, left panel, and data not shown); this lower proliferation rate correlated with a moderate degree of p53 activation in the same cells. In fact, analysis of the status of p53 activity revealed a slight increase of p53 phosphorylation (Ser 18) and p21 expression in the $NPM^{-/-}$ cultures (Fig. 2D, middle panel). Notably, reexpression of NPM into $NPM^{-/-}$ hematopoietic precursors (by retroviral gene transfer) reduced levels of p53 phosphorylation and p21 expression and restored the efficiency of colony formation (Fig. 2D). Together, these findings indicate that $NPM^{-/-}$ cells can be grown in culture only if p53 is lost, as in the $p53^{-/-}$ $NPM^{-/-}$ MEFs, or functionally inhibited, as occurs with $NPM^{-/-}$ yolk sac cells when grown in the presence of cytokines.

p53 activation in $NPM^{-/-}$ cells is part of a DNA damage response. We next investigated the mechanisms responsible for p53 activation in $NPM^{-/-}$ cells. It has been proposed that NPM inhibits p53-dependent Arf activity by targeting it to nucleoli, thus segregating Arf from p53 (20). To test whether activation of p53 in $NPM^{-/-}$ cells is due to Arf activation, we down-regulated expression of NPM in $Arf^{-/-}$ MEFs, using lentivirus vectors expressing NPM-specific short hairpin RNAs. Down-regulation of NPM expression in $Arf^{-/-}$ cells (Fig. 3A) led to increased p53 stabilization (Fig. 3A), accumulation of p21 (Fig. 3A), and decreased cellular growth (Fig. 3B), demonstrating that Arf is not critical for activation of p53 following NPM depletion.

Activation of p53 is part of a checkpoint response to DNA damage, which involves activation of ATM/ATR kinases, phosphorylation of a set of downstream targets, including histone H2AX, and their accumulation at sites of DNA double-strand breaks or stalled replication forks (14). Western blotting analysis of H2AX phosphorylation (γ-H2AX) in total embryo lysates revealed higher level of γ-H2AX in the $NPM^{-/-}$ samples compared to wild-type samples (Fig. 3C). immunohistochemistry analysis of various embryo tissues confirmed markedly increased γ-H2AX focus formation in the $NPM^{-/-}$ samples (Fig. 3D for representative sections). Likewise, Western blotting (Fig. 3C) and immunofluorescence (Fig. 3E) experiments revealed increased levels of γ-H2AX and γ-H2AX focus formation in cultured $NPM^{-/-}$ yolk cells compared to the wild-type samples. Staining of yolk sac cells with antibodies against phosphorylated ATM revealed the presence of phosphorylated ATM foci in the $NPM^{-/-}$ but not wild-type cells, which largely colocalized with the γ-H2AX foci (Fig. 3F). Notably, reexpression of NPM in $NPM^{-/-}$ yolk cells restored levels of γ-H2AX and phosphorylated ATM foci to the background levels of wild-type cells (Fig. 3F and 3C). It appears, therefore, that loss of NPM leads to the constitutive activation of a DNA damage response, suggesting that p53 activation in $NPM^{-/-}$ cells is secondary to the loss of a checkpoint function of NPM on DNA integrity.

Increased cell proliferation in $NPM^{-/-}$ embryos and double-knockout MEFs. We then investigated the effects of NPM expression on cellular proliferation by measuring BrdU incorporation in wild-type and $NPM^{-/-}$ embryos and comparing the growth properties of double-knockout and $p53^{-/-}$ MEFs. To analyze BrdU incorporation in embryos, 10.5 dpc pregnant female mice were intraperitoneally injected with BrdU and

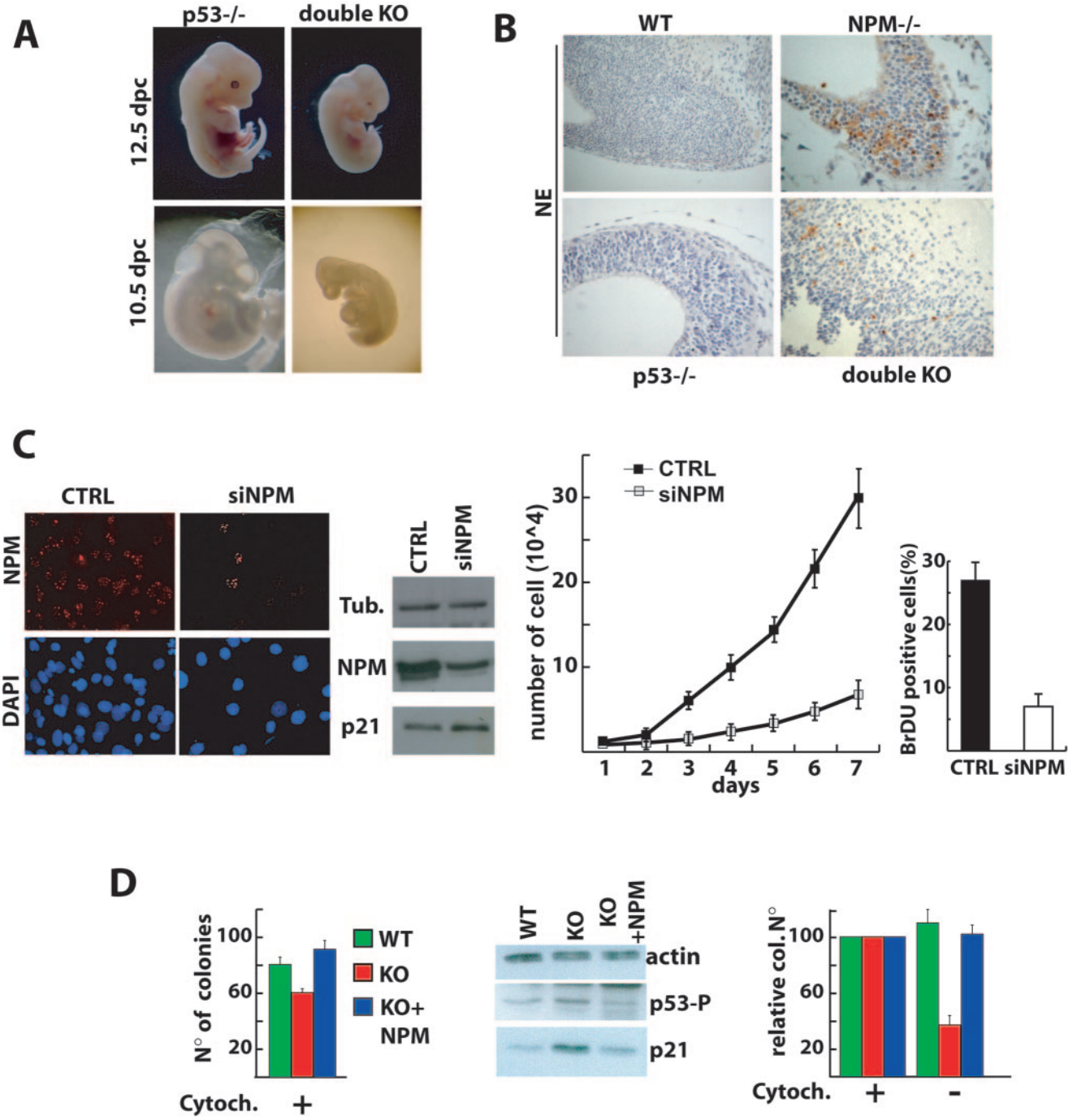

FIG. 2. Loss of p53 gene rescues apoptosis in NPM knockout (KO) embryos. (A) $p53^{-/-}$ and double-knockout ($p53^{-/-}$ $NPM^{-/-}$) embryos at different stages of development (10.5 and 12.5 dpc). (B) Analysis of apoptosis in the developing neuroepithelium (NE) of wild-type (WT), $NPM^{-/-}$, $p53^{-/-}$ and double-knockout embryos. Immunohistochemistry analysis was performed using anti-activated caspase-3 antibody and counterstained with hematoxylin end eosin. (C) Down-regulation of NPM expression in wild-type MEFs by short interfering RNA. Cells were infected with a control (CTRL) lentivirus or a lentivirus expressing short interfering RNA for NPM (siNPM), as indicated, and analyzed by immunofluorescence using an anti-NPM antibody (NPMa) and by Western blot using anti-NPM and anti-p21 antibodies. For the growth curves, infected cells were seeded on six-well plates at a density of 10^4 cells per well. Cultures were harvested every day, and the number of cells was determined. The numbers refer to mean values of triplicate determinations. At day 3 of the growth curve, levels of BrdU incorporation were determined by FACS analysis (results refers to mean values of triplicate determinations). (D) Left panel: 2,000 cells derived from the yolk sac of knockout and wild-type embryos and knockout embryos reconstituted with GFP-NPM were seeded in semisolid medium supplemented with interleukin-3, interleukin-6, and stem cell factor and scored after 10 days for number of colonies. Middle panel: expression of phosphorylated p53 (anti-Ser18) and its target p21 in yolk sac-derived cells. Right panel: yolk sac-derived cells were cultured in suspension for 24 h, with (control) or without cytokines, and counted after 10 days (results are expressed as a percentage of the colonies obtained with control cells).

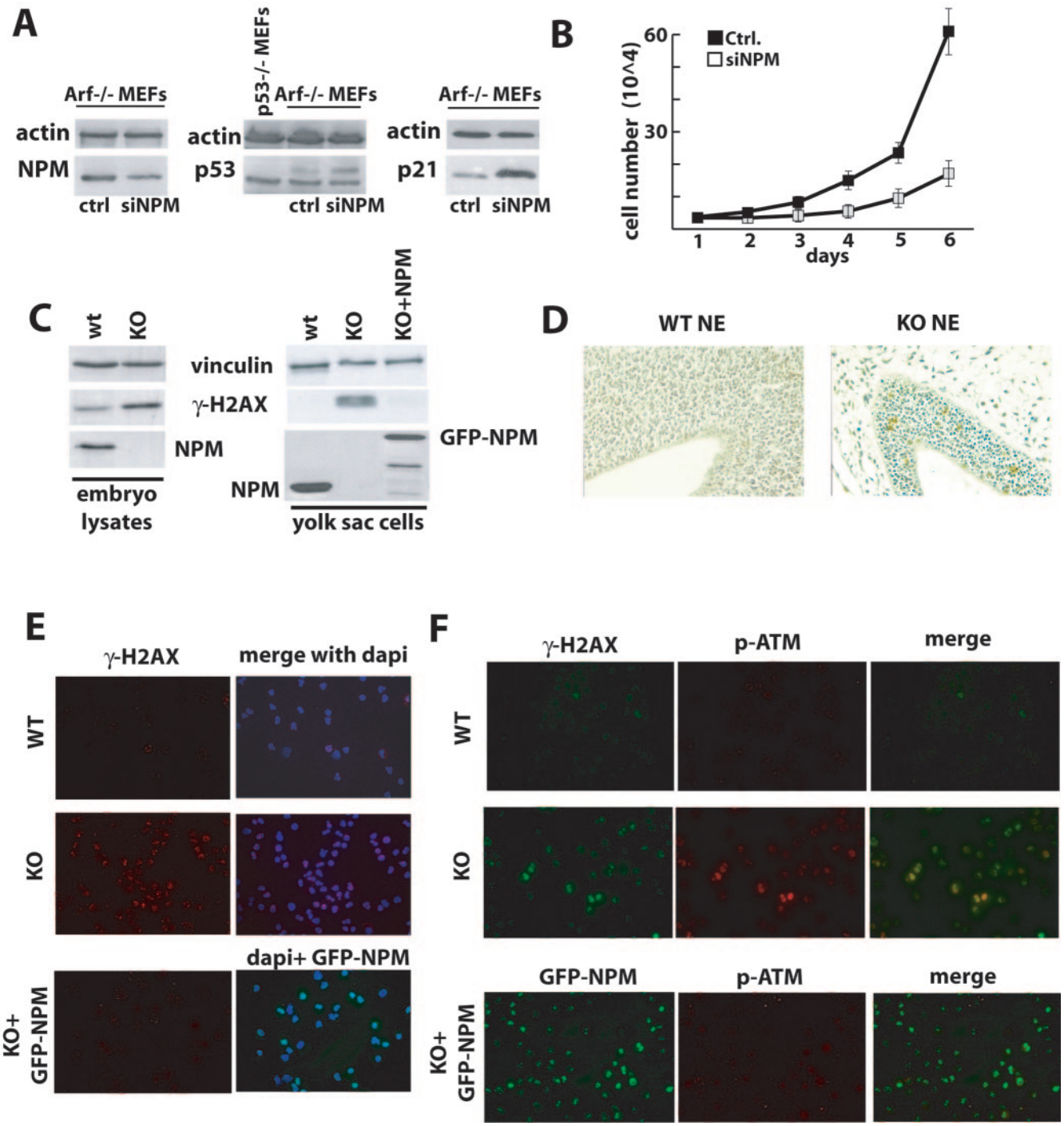

FIG. 3. p53 activation in NPM null cells is part of a DNA damage response. (A) Western blots of lysates from the same cells as in panel B analyzed with antibodies against NPM, p21, and p53. (B) Growth curves of $Arf^{-/-}$ MEFs infected with a control lentivirus or a lentivirus expressing short interfering RNA for NPM (siNPM); 2×10^4 cells were plated in six-well plates. Cultures were harvested every day, and the number of cells was determined. The numbers refer to mean values of triplicate determinations. (C) Western blotting analysis of γH2AX expression in lysates of total embryo and yolk sac cells. (D) Analysis of γH2AX expression in the developing brain of wild-type (WT) NPM and knockout (KO) 10.5 dpc embryos. Embryo sections were stained with a monoclonal antibody against the phosphorylated form of H2AX and counterstained with hematoxylin and eosin. (E and F) Immunofluorescence analysis of γH2AX and phosphorylated ATM (p-ATM) expression in wild-type and knockout yolk sac cells and in knockout cells reconstituted with GFP-NPM.

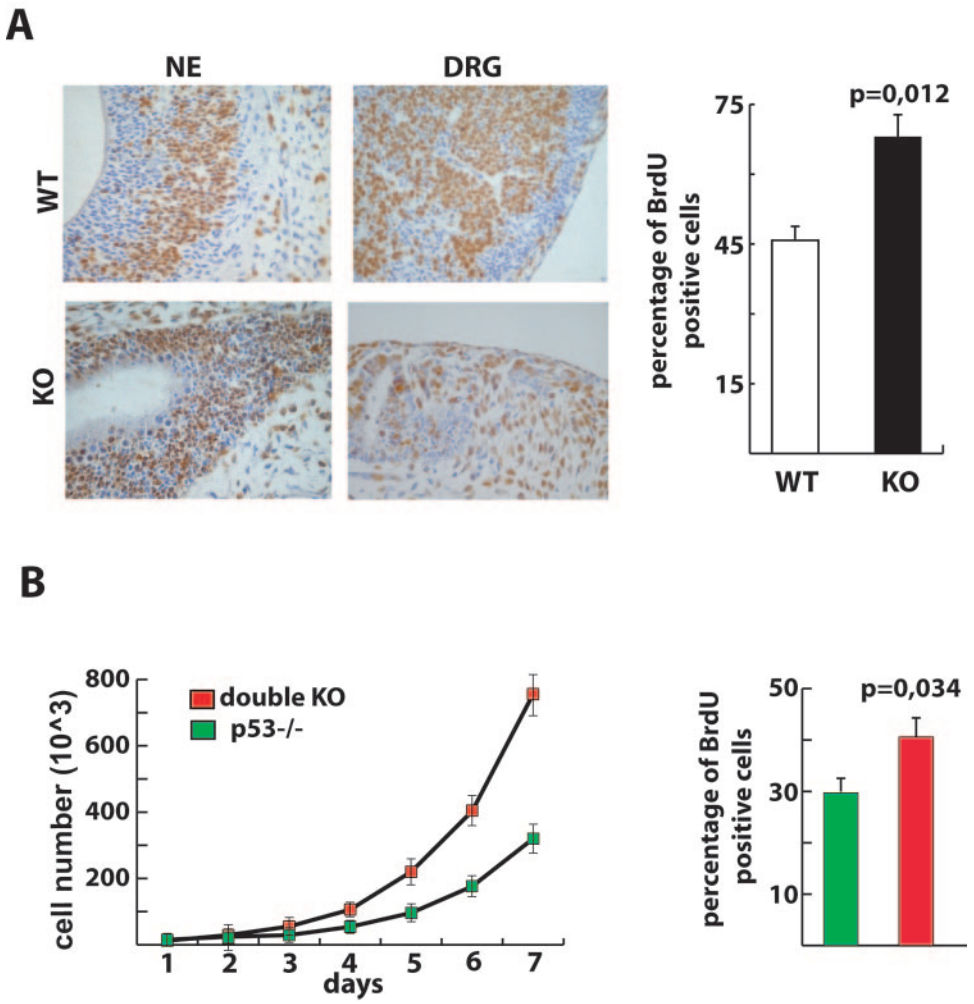

FIG. 4. Loss of NPM leads to increased proliferation. (A) Left panel: immunohistochemistry analysis of proliferation (anti-BrdU staining) in the developing neuroepithelium and dorsal root ganglia (DRG) of wild-type (WT) NPM and knockout (KO) 10.5 dpc embryos. Right panel: evaluation of BrdU-positive cells in wild-type and knockout embryos through FACS analysis of cells derived directly from embryos after treatment with 0.1% collagenase. (B) Right panel: growth curves of $p53^{-/-}$ and double-knockout MEFs at passage 4 (2×10^4 cells were plated into six-well plates). Cultures were harvested every day, and the total number of cells was determined. The numbers represent the mean values of triplicate determinations. The experiment was repeated twice, using two independently derived MEF cultures, and gave comparable results. Left panels: evaluation of BrdU-positive cells in growing $p53^{-/-}$ and double-knockout MEFs. Bars represent mean values of triplicate determinations. The experiments were repeated three times, giving comparable results.

sacrificed 45 min later. The recovered embryos were analyzed for BrdU incorporation in situ by immunohistochemistry.

Microscopic examination of embryo sections from different tissues revealed a random dispersion of BrdU-positive cells in the mutant tissues, at variance with their normal counterparts, where cycling and resting cells typically cluster within separate areas (Fig. 4A for representative sections from neuroepithelium and dorsal root ganglia). Analysis of the frequency of BrdU-positive cells revealed a slightly yet consistently higher number of cycling cells in the $NPM^{-/-}$ samples than in the wild-type counterparts (Fig. 4A). To obtain a quantitative estimate of BrdU positivity, we performed a FACS analysis of cell suspensions obtained from wild-type and $NPM^{-/-}$ embryos of different stage (E9.5 and 10.5 dpc). The results showed an approximately 45% increase of BrdU-positive cells in $NPM^{-/-}$ embryos (see Fig. 4A for representative results obtained from 10.5 dpc embryos). Together, these data demonstrate that NPM expression is not critical for cell cycle progression, as previously hypothesized (15), and that, on the contrary, it negatively regulates progression through the cell cycle.

Comparison of the growth properties of double-knockout and $p53^{-/-}$ MEFs revealed that double-knockout fibroblasts grow markedly faster than $p53^{-/-}$ controls (see Fig. 4B for one representative curve). BrdU incorporation analysis performed on logarithmically growing cell population revealed an approximately 35% increase of BrdU-positive cells in the double-knockout cells (Fig. 4B). It appears, therefore, that loss of NPM expression correlates with increased proliferation both in vivo and in cultured cells. In the latter, however, increased proliferation can only be observed if p53 is lost, since the loss of NPM is also responsible for the activation of a p53-depen-

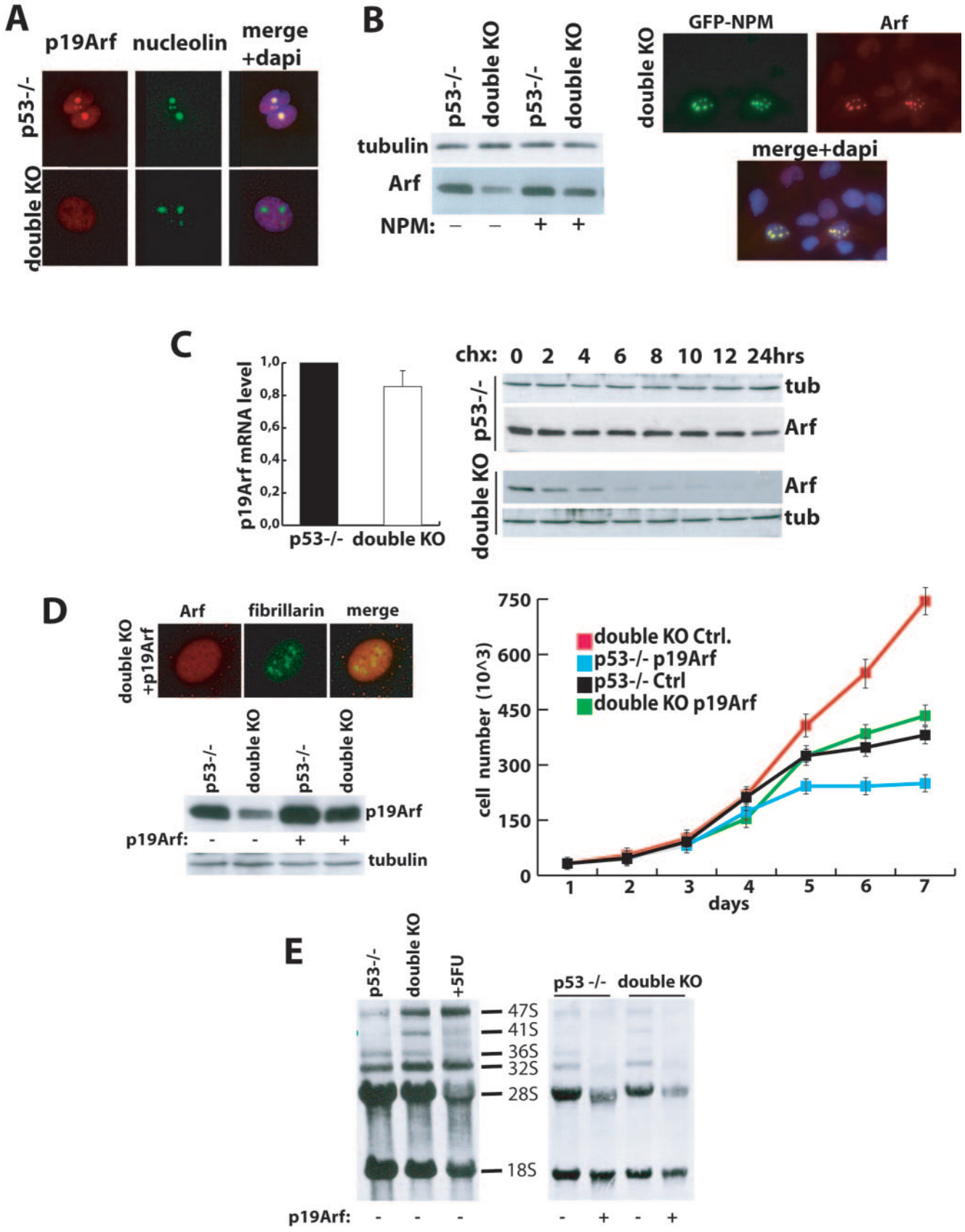

FIG. 5. Regulation of Arf stability and function by NPM. (A) Immunofluorescence analysis of $p19^{Arf}$ localization (red) in $p53^{-/-}$ and double-knockout (KO) MEFs. Nucleolin staining (green) was used as a marker for nucleoli. (B) Left panels: Western blotting analysis of $p19^{Arf}$

dent checkpoint. Whether, in the NPM$^{-/-}$ fibroblasts, the increased proliferation is responsible for the accumulation of DNA replication alterations, which then activate a (p53-dependent) intra-S-phase checkpoint (1) remains, however, to be determined.

NPM is critical for the nucleolar localization and stability of Arf protein. Arf inhibits cell proliferation through both p53-dependent and -independent mechanisms (34). Since NPM physically interacts with Arf and protects it from degradation (20), the inhibitory effect of NPM on cellular proliferation might be mediated by Arf itself. Therefore, we investigated the effects of NPM on Arf expression. Immunofluorescence analysis of p53$^{-/-}$ and p53$^{-/-}$ NPM$^{-/-}$ (double-knockout) MEFs revealed that Arf, in the absence of NPM, is nuclear-diffuse and completely excluded from nucleoli, which remain as intact organelles, as shown by staining with other nucleolar markers, such as nucleolin (Fig. 5A) and fibrillarin (not shown). Notably, Arf levels in the double-knockout MEFs were markedly lower than in the control p53$^{-/-}$ MEFs (Fig. 5B, left panel). Reexpression of NPM in double-knockout cells restored normal levels (Fig. 5B), compared to p53$^{-/-}$ cells, and nucleolar localization of Arf (Fig. 5B).

Since levels of *arf* mRNA were comparable in the p53$^{-/-}$ and double-knockout MEFs (Fig. 5C, left panel), we investigated whether NPM regulates Arf stability. To this end, p53$^{-/-}$ and double-knockout cells were exposed to 100 μM cycloheximide to inhibit de novo protein synthesis, harvested at serial time points following treatment, and assessed for Arf levels by Western blotting. The half-life of Arf in p53$^{-/-}$ MEFs was approximately 12 h (Fig. 5C, right panel). In the double-knockout cells the stability of the Arf protein was markedly reduced, with a half-life of about 2 to 4 h (Fig. 5C, right panel). Therefore, NPM is indispensable for the nucleolar localization of Arf and critical for its stability. These data are consistent with previous reports showing destabilization and partial delocalization of Arf following down-regulation of NPM expression (20).

NPM is not a downstream target of Arf. Upon activation by abnormally high thresholds of mitogenic signals, such as those imposed by oncogenic Myc or Ras, Arf activates p53 via Mdm2, enabling cells to stop proliferating (35). Arf can inhibit ribogenesis (36) and, though less efficiently, suppress proliferation of cells that lack both p53 and Mdm2, implying interaction with other regulators (39). Due to its reported properties of stimulating the cell cycle and ribogenesis, NPM has been proposed as a critical downstream target of Arf (18). Upon activation, Arf would bind NPM directly, thus inducing its degradation or blocking its nucleus-cytoplasm shuttling activity (7). Therefore, we evaluated the effects of NPM on the ability of Arf to inhibit cellular growth and ribosome biogenesis in p53$^{-/-}$ cells.

p53$^{-/-}$ and double-knockout MEFs infected with control or Arf-expressing retroviruses were analyzed for proliferation capacity or labeled with [^{3}H]uridine in order to evaluate newly synthesized rRNA. Exogenously expressed Arf localized predominantly within nucleoli in the p53$^{-/-}$ MEFs, as expected (not shown), while it was nuclear diffuse and mainly excluded from nucleoli in the double-knockout cells (Fig. 5D). Consistent with the observed effect of NPM on Arf stability, levels of exogenous Arf were lower in double-knockout than in p53$^{-/-}$ cells (Fig. 4D). The ability of overexpressed Arf to reduce cell proliferation was comparable in p53$^{-/-}$ and double-knockout MEFs (Fig. 5D). Notably, the proliferation rate of the various MEF populations (controls and p19^{Arf} infected) nicely correlated with the levels of p19^{Arf} (Fig. 4D). As an example, p19^{Arf}-infected double-knockout cells and p53$^{-/-}$ control cells expressed comparable levels of p19^{Arf} and showed similar growth rates (Fig. 5D). Finally, the ability of overexpressed Arf to reduce maturation of the 28S rRNA was comparable in p53$^{-/-}$ and double-knockout MEFs (Fig. 5E). The effect of NPM expression on rRNA processing was also negligible under basal conditions (Fig. 5E). It appears, therefore, that expression of NPM is not rate limiting for rRNA processing and that the ability of ectopically overexpressed Arf to inhibit ribogenesis and cellular proliferation (in the absence of p53) is independent of NPM and its nucleolar localization.

NPM regulates the biological activities of Arf. Mitogenic stimuli, as imposed by enforced expression of c-Myc or the RasV12 mutant, induce expression of Arf, which leads to p53 stabilization. The absence of p53 and/or Arf expression suppresses this phenotype and increases the chances of cellular transformation (12). Moreover, Arf inhibits Myc through direct binding, independently of its function on p53 (29). Therefore, to investigate the functions of Arf that are p53 independent, we ectopically expressed c-Myc in p53$^{-/-}$ and double-knockout MEFs. Expression of Myc in p53$^{-/-}$ MEFs increased the rate of cell proliferation (Fig. 6A) and induced their oncogenic conversion, as measured by the ability of Myc-expressing cells to form colonies in semisolid medium (Fig. 6A). Comparable levels of overexpressed Myc (Fig. 6A) provoked, in the double-knockout MEFs, a higher proliferation rate and increased frequency of transformation (Fig. 6A). Notably, the size of methylcellulose colonies formed by the double-knock-

protein levels in p53$^{-/-}$ and double-knockout MEFs either under basal conditions or after infection with a GFP-NPM-expressing retrovirus (NPM). Right panels: immunofluorescence analysis of GFP-NPM localization in double-knockout MEFs (green) and its effect on endogenous p19^{Arf} localization (red). (C) Left panel: p19^{Arf} mRNA levels in p53$^{-/-}$ and double-knockout MEFs evaluated by quantitative PCR analysis (results are normalized against p53$^{-/-}$ RNA). Right panel: Western blotting analysis of p19^{Arf} protein stability in p53$^{-/-}$ and double-knockout MEFs. MEFs were treated with cycloheximide (chx) to block protein synthesis and analyzed at the indicated time points after wash-out. As an internal control, the same lysates were probed with antibodies against tubulin, which is stable over the 24 h of the experimental procedure. (D) Upper left panel: immunofluorescence analysis of double-knockout MEFs infected with a p19^{Arf}-expressing retroviruses. Lower left panel: Western blotting analysis of p19^{Arf} protein levels in double-knockout and p53$^{-/-}$ MEFs infected with a control retrovirus or a retrovirus expressing p19^{Arf}. Right panel: growth curves of p53$^{-/-}$ and double-knockout MEFs infected with a control retrovirus or a retrovirus expressing p19^{Arf}; 2×10^4 cells were plated into six-well plates and counted at daily intervals. Numbers refer to the mean values of triplicate determinations. (E) Evaluation of newly synthesized rRNA by pulse-chase labeling with [^{3}H]uridine in uninfected double-knockout and p53$^{-/-}$ MEFs (left panel) or upon infection with a control retrovirus or with a p19^{Arf}-expressing retrovirus (right panel). Double-knockout MEFs were treated with 5-fluorouracil (5FU), as indicated. The different rRNA species, as detected by autoradiography, are indicated between the two panels.

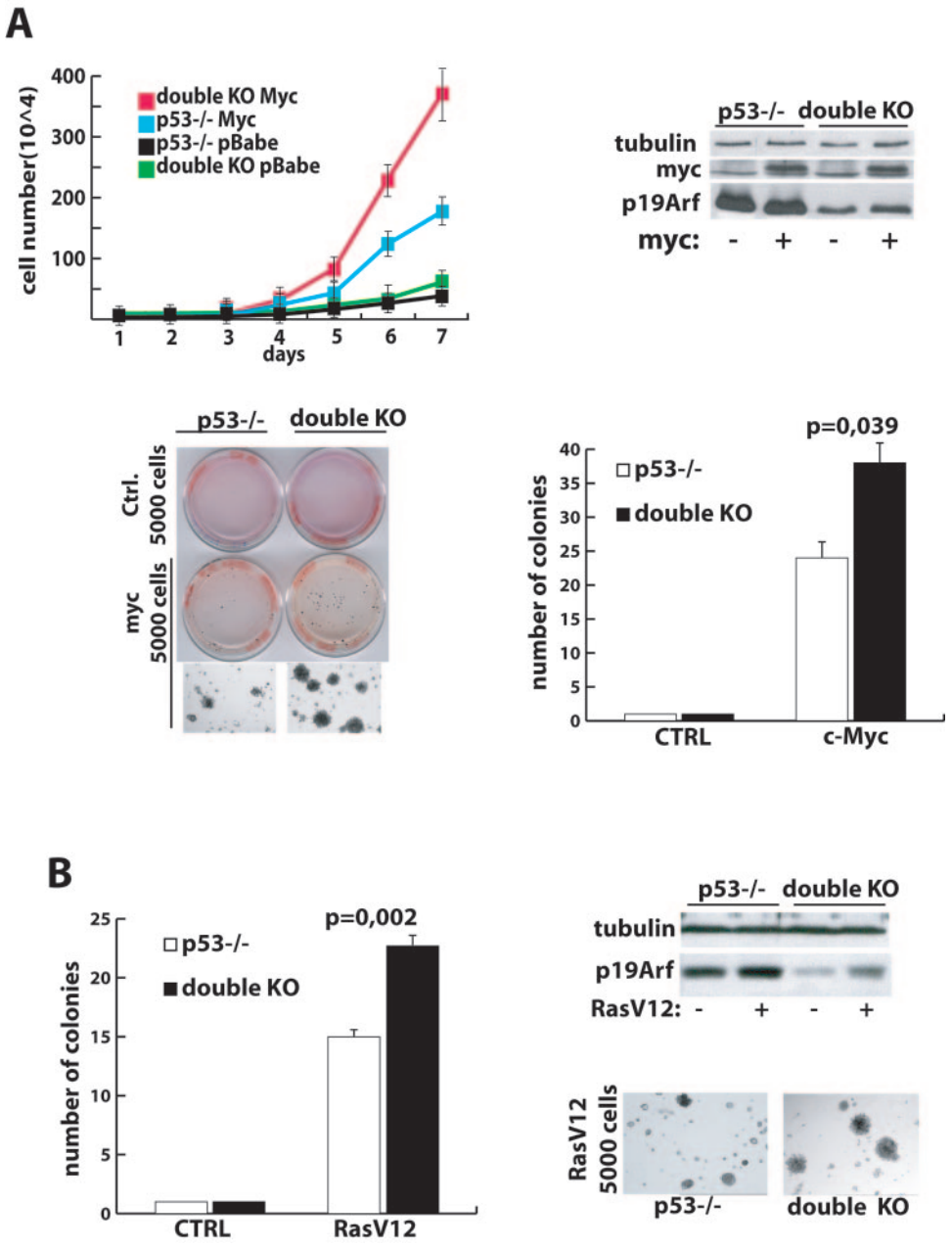

FIG. 6. Effects of NPM expression on transformation by Myc and Ras. (A) $p53^{-/-}$ and double-knockout (KO) MEFs were infected with a control retrovirus or a retrovirus expressing the c-*myc* oncogene. At the end of the selection, 2×10^4 cells were plated into six-well plates and cells were counted at daily intervals. The numbers refer to the mean values of triplicate determinations. The same cells were analyzed by Western blotting using antibodies against tubulin, $p19^{Arf}$ and Myc (right upper panel) and plated in semisolid medium (in triplicate). The number of colonies (right lower panel) and representative plates and colonies (left lower panels) are shown. (C) Same experiment as described for panel A, using a retrovirus expressing the RasV12 oncogene. We evaluated tubulin and $p19^{Arf}$ protein levels (right upper panel) and numbers of colonies formed after plating in semisolid medium (left panel). Representative colonies are also shown (right lower panel).

out cells was considerably larger than that of the controls (Fig. 6A). Comparable results, in terms of transforming ability and colony growth, have been obtained by infecting the same cells with RasV12 (Fig. 5B). In the cases of both RasV12 and Myc, oncogene-induced Arf stabilization was modest in the double-knockout MEFs, and $p19^{Arf}$ levels remain markedly lower than in the $p53^{-/-}$ MEFs.

Taken together, these results indicate that, in the absence of NPM, the p53-independent effects of Arf on cellular proliferation are less potent, either under basal conditions or after oncogenic stimuli, likely due to reduced stability of the Arf protein.

DISCUSSION

We have demonstrated that the loss of NPM expression provokes activation of a DNA damage response, suggesting

that one physiological function of NPM is to ensure DNA integrity. This is consistent with earlier work showing the involvement of NPM in the process of DNA repair after treatment with different DNA-damaging agents, including UV light (41). How NPM participates in DNA repair is not fully understood. NPM is part of a multiprotein complex that possesses DNA recombination activity on immunoglobulin heavy-chain switch region sequences (5). In vitro, NPM promotes DNA single-strand reannealing and mediates D-loop formation (5), suggesting that it may participate in the first steps of a recombination reaction (pairing of DNA substrates, strand invasion, and formation of stable joint molecules). Alternatively, NPM might function as a histone chaperone after DNA lesions are repaired, during the assembly of new nucleosomes. In fact, NPM binds histones and favors nucleosome assembly in vitro (26).

Due to accumulation of damaged DNA, cells lacking NPM activate a DNA damage response, which involves p53 activation and leads to senescence or apoptosis. In fact, fibroblasts explanted from $NPM^{-/-}$ embryos undergo growth arrest when grown in culture, while fibroblasts from $p53^{-/-}$ $NPM^{-/-}$ embryos can be easily propagated in culture. The availability of double-knockout fibroblasts allowed us to investigate the effect of NPM expression on cellular growth. Clearly, NPM expression is not critical for ribogenesis and cell proliferation. Double-knockout fibroblasts grow faster than control cells and are more susceptible to transformation by activated oncogenes, such as RasV12 or c-*myc*. Notably, we also found increased numbers of proliferating cells in the $NPM^{-/-}$ embryos, suggesting that one additional function of NPM is to inhibit cellular proliferation.

The inhibitory effect exerted by NPM on cell proliferation might be mediated by Arf. Arf protein is polyubiquitinated at its N terminus and its degradation depends on the ubiquitin-proteasome pathway (21). NPM binds the Arf protein and protects it from degradation (21). Indeed, the stability of Arf protein is markedly decreased in cells that lack NPM expression. However, inhibition of the proteasome only partially restores the stability of $p19^{Arf}$ mutants that do not bind NPM (21), suggesting that NPM protects Arf from both proteasome-dependent and -independent degradation.

The amino-terminal region of Arf is dynamically disordered in aqueous solution and becomes highly structured upon binding to Mdm2, suggesting that, in vivo, Arf is an intrinsically unstructured protein that folds on binding to its biological substrates (6). NPM might bind newly synthesized Arf and serve as a molecular chaperone to favor acquisition of a tertiary and stable structure, thus preventing its degradation or aggregation.

However, when complexed to NPM, Arf maintains a free N terminus and can be ubiquitinated (21). The leukemia-associated NPM mutant retains the ability to interact with Arf, but it fails to prevent its degradation. Notably, this mutant is unable to enter the nucleus and localizes mainly in the cytoplasm, suggesting that one mechanism through which NPM protects Arf from degradation is by ensuring its proper nucleolar or nucleoplasmic localization.

Whether these two activities of NPM, regulation of DNA integrity and of Arf protein stability, are functionally linked remains unknown. DNA-damaging agents provoke the mobilization of nucleolar NPM into the nucleoplasm (22), and its binding to chromatin (28). Oncogene expression induces upregulation of Arf and, like the DNA-damaging agents, the partial nucleoplasmic mobilization of NPM (9). NPM, in turn, is indispensable for the full stabilization of Arf proteins after oncogene expression. Recent findings indicate that oncogene-driven cell divisions induce a DNA damage response which might be responsible for activation of the Arf-p53 pathway after oncogene expression (2). Thus, NPM might function as specialized chaperone in the cellular response to DNA damage, to coordinate arrest of cell proliferation and DNA repair through its effects on Arf stability and chromatin, respectively.

Regardless of the underlying molecular mechanisms, these activities of NPM might be relevant for the inherent ability of cells to suppress transformation. NPM is frequently mutated in leukemias (13) and lymphomas (24), suggesting that inactivation of the putative NPM tumor suppressor activities might be critical for transformation. The leukemia-associated NPM mutant competes with wild-type NPM in binding Arf, is unable to protect it from degradation, and provokes its delocalization in the cytoplasm (submitted for publication). Thus, in leukemias carrying a mutated NPM allele, the levels of Arf protein are decreased and the protein itself is delocalized, suggesting that mutations of NPM lead to functional inactivation of the Arf tumor suppressor pathway.

ACKNOWLEDGMENTS

We thank B. Amati for many helpful discussions and critical reading of the manuscript. NPM-deficient mice were generated by Lexicon Genetics Inc. (The Woodlands, TX).

This work was supported by grants to P.G.P. from AIRC, MIUR, and EC.

REFERENCES

1. **Bartek, J., C. lukas, and J. Lukas.** 2004. Checking on DNA damage in S phase. Nat. Rev. Mol. Cell. Biol. **5:**792–804.
2. **Bartkova, J., Z. Horejsi, K. Koed, A. Kramer, F. Tort, K. Zieger, P. Guldberg, M. Sehested, J. M. Nesland, C. Lukas, T. Orntoft, J. Lukas, and J. Bartek.** 2005. DNA damage response as a candidate anti-cancer barrier in early human tumorigenesis. Nature **434:**864–870.
3. **Bertwistle, D., M. Sugimoto, and C. J. Sherr.** 2004. Physical and functional interactions of the Arf tumor suppressor protein with nucleophosmin/B23. Mol. Cell. Biol. **24:**985–996.
4. **Borer, R. A., C. F. Lehner, H. M. Eppenberger, and E. A. Nigg.** 1989. Major nucleolar proteins shuttle between nucleus and cytoplasm. Cell **56:**379–390.
5. **Borggrefe, T., M. Wabl, A. T. Akhmedov, and R. Jessberger.** 1998. A B-cell-specific DNA recombination complex. J. Biol. Chem. **273:**17025–17035.
6. **Bothner, B., W. S. Lewis, E. L. DiGiammarino, J. D. Weber, S. J. Bothner, and R. W. Kriwacki.** 2001. Defining the molecular basis of Arf and Hdm2 interactions. J. Mol. Biol. **314:**263–277.
7. **Brady, S. N., Y. Yu, L. B. Maggi, Jr., and J. D. Weber.** 2004. ARF impedes NPM/B23 shuttling in an Mdm2-sensitive tumor suppressor pathway. Mol. Cell. Biol. **24:**9327–9338.
8. **Chan, W. Y., Q. R. Liu, J. Borjigin, H. Busch, O. M. Rennert, L. A. Tease, and P. K. Chan.** 1989. Characterization of the cDNA encoding human nucleophosmin and studies of its role in normal and abnormal growth. Biochemistry **28:**1033–1039.
9. **Colombo, E., J. C. Marine, D. Danovi, B. Falini, and P. G. Pelicci.** 2002. Nucleophosmin regulates the stability and transcriptional activity of p53. Nat. Cell Biol. **4:**529–533.
10. **Cordell, J. L., K. A. Pulford, B. Bigerna, G. Roncador, A. Banham, E. Colombo, P. G. Pelicci, D. Y. Mason, and B. Falini.** 1999. Detection of normal and chimeric nucleophosmin in human cells. Blood **93:**632–642.
11. **Dumbar, T. S., G. A. Gentry, and M. O. Olson.** 1989. Interaction of nucleolar phosphoprotein B23 with nucleic acids. Biochemistry **28:**9495–9501.
12. **Eischen, C. M., J. D. Weber, M. F. Roussel, C. J. Sherr, and J. L. Cleveland.** 1999. Disruption of the ARF-Mdm2-p53 tumor suppressor pathway in Myc-induced lymphomagenesis. Genes Dev. **13:**2658–2669.
13. **Falini, B., C. Mecucci, E. Tiacci, M. Alcalay, R. Rosati, L. Pasqualucci, R. La Starza, D. Diverio, E. Colombo, A. Santucci, B. Bigerna, R. Pacini, A.**

Pucciarini, A. Liso, M. Vignetti, P. Fazi, N. Meani, V. Pettirossi, G. Saglio, F. Mandelli, F. Lo-Coco, P. G. Pelicci, and M. F. Martelli. 2005. Cytoplasmic nucleophosmin in acute myelogenous leukemia with a normal karyotype. N. Engl. J. Med. **352:**254–266.

14. **Fernandez-Capetillo, O., A. Celeste, and A. Nussenzweig.** 2003. Focusing on foci: H2AX and the recruitment of DNA-damage response factors. Cell Cycle **2:**426–427.
15. **Feuerstein, N., and J. J. Mond.** 1987. "Numatrin," a nuclear matrix protein associated with induction of proliferation in B lymphocytes. J. Biol. Chem. **262:**11389–11397.
16. **Giaccia, A. J., and M. B. Kastan.** 1998. The complexity of p53 modulation: emerging patterns from divergent signals. Genes Dev. **12:**2973–2983.
17. **Hsu, C. Y., and B. Y. Yung.** 1998. Down-regulation of nucleophosmin/B23 during retinoic acid-induced differentiation of human promyelocytic leukemia HL-60 cells. Oncogene **16:**915–923.
18. **Itahana, K., K. P. Bhat, A. Jin, Y. Itahana, D. Hawke, R. Kobayashi, and Y. Zhang.** 2003. Tumor suppressor ARF degrades B23, a nucleolar protein involved in ribosome biogenesis and cell proliferation. Mol. Cell **12:**1151–1164.
19. **Jacks, T., L. Remington, B. O. Williams, E. M. Schmitt, S. Halachmi, R. T. Bronson, and R. A. Weinberg.** 1994. Tumor spectrum analysis in p53-mutant mice. Curr. Biol. **4:**1–7.
20. **Korgaonkar, C., J. Hagen, V. Tompkins, A. A. Frazier, C. Allamargot, F. W. Quelle, and D. E. Quelle.** 2005. Nucleophosmin (B23) targets ARF to nucleoli and inhibits its function. Mol. Cell. Biol. **25:**1258–1271.
21. **Kuo, M. L., W. den Besten, D. Bertwistle, M. F. Roussel, and C. J. Sherr.** 2004. N-terminal polyubiquitination and degradation of the Arf tumor suppressor. Genes Dev. **18:**1862–1874.
22. **Kurki, S., K. Peltonen, L. Latonen, T. M. Kiviharju, P. M. Ojala, D. Meek, and M. Laiho.** 2004. Nucleolar protein NPM interacts with HDM2 and protects tumor suppressor protein p53 from HDM2-mediated degradation. Cancer Cell **5:**465–475.
23. **Maiguel, D. A., L. Jones, D. Chakravarty, C. Yang, and F. Carrier.** 2004. Nucleophosmin sets a threshold for p53 response to UV radiation. Mol. Cell. Biol. **24:**3703–3711.
24. **Morris, S. W., M. N. Kirstein, M. B. Valentine, K. G. Dittmer, D. N. Shapiro, D. L. Saltman, and A. T. Look.** 1994. Fusion of a kinase gene, ALK, to a nucleolar protein gene, NPM, in non-Hodgkin's lymphoma. Science **263:**1281–1284. (Erratum, 267:316–317.)
25. **Nozawa, Y., N. Van Belzen, A. C. Van der Made, W. N. Dinjens, and F. T. Bosman.** 1996. Expression of nucleophosmin/B23 in normal and neoplastic colorectal mucosa. J. Pathol. **178:**48–52.
26. **Okuwaki, M., K. Matsumoto, M. Tsujimoto, and K. Nagata.** 2001. Function of nucleophosmin/B23, a nucleolar acidic protein, as a histone chaperone. FEBS Lett. **506:**272–276.
27. **Olson, M. O., M. O. Wallace, A. H. Herrera, L. Marshall-Carlson, and R. C. Hunt.** 1986. Preribosomal ribonucleoprotein particles are a major component of a nucleolar matrix fraction. Biochemistry **25:**484–491.
28. **Paron, I., A. D'Elia, C. D'Ambrosio, A. Scaloni, F. D'Aurizio, A. Prescott, G. Damante, and G. Tell.** 2004. A proteomic approach to identify early molecular targets of oxidative stress in human epithelial lens cells. Biochem. J. **378:**929–937.
29. **Qi, Y., M. A. Gregory, Z. Li, J. P. Brousal, K. West, and S. R. Hann.** 2004. p19ARF directly and differentially controls the functions of c-Myc independently of p53. Nature **431:**712–717.
30. **Quelle, F. W., J. Wang, J. Feng, D. Wang, J. L. Cleveland, J. N. Ihle, and G. P. Zambetti.** 1998. Cytokine rescue of p53-dependent apoptosis and cell cycle arrest is mediated by distinct Jak kinase signaling pathways. Genes Dev. **12:**1099–1107.
31. **Rubinson, D. A., C. P. Dillon, A. V. Kwiatkowski, C. Sievers, L. Yang, J. Kopinja, D. L. Rooney, M. M. Ihrig, M. T. McManus, F. B. Gertler, M. L. Scott, and L. Van Parijs.** 2003. A lentivirus-based system to functionally silence genes in primary mammalian cells, stem cells and transgenic mice by RNA interference. Nat. Genet. **33:**401–406.
32. **Ryan, K. M., A. C. Phillips, and K. H. Vousden.** 2001. Regulation and function of the p53 tumor suppressor protein. Curr. Opin. Cell Biol. **13:**332–337.
33. **Savkur, R. S., and M. O. Olson.** 1998. Preferential cleavage in pre-ribosomal RNA by protein B23 endoribonuclease. Nucleic Acids Res. **26:**4508–4515.
34. **Sherr, C. J.** 2001. The INK4a/ARF network in tumour suppression. Nat. Rev. Mol. Cell. Biol. **2:**731–737.
35. **Sherr, C. J., and J. D. Weber.** 2000. The ARF/p53 pathway. Curr. Opin. Genet. Dev. **10:**94–99.
36. **Sugimoto, M., M. L. Kuo, M. F. Roussel, and C. J. Sherr.** 2003. Nucleolar Arf tumor suppressor inhibits ribosomal RNA processing. Mol. Cell **11:**415–424.
37. **Szebeni, A., and M. O. Olson.** 1999. Nucleolar protein B23 has molecular chaperone activities. Protein Sci. **8:**905–912.
38. **Vousden, K. H., and X. Lu.** 2002. Live or let die: the cell's response to p53. Nat. Rev. Cancer **2:**594–604.
39. **Weber, J. D., J. R. Jeffers, J. E. Rehg, D. H. Randle, G. Lozano, M. F. Roussel, C. J. Sherr, and G. P. Zambetti.** 2000. p53-independent functions of the p19(ARF) tumor suppressor. Genes Dev. **14:**2358–2365.
40. **Wu, M. H., J. H. Chang, C. C. Chou, and B. Y. Yung.** 2002. Involvement of nucleophosmin/B23 in the response of HeLa cells to UV irradiation. Int. J. Cancer **97:**297–305.
41. **Wu, M. H., J. H. Chang, and B. Y. Yung.** 2002. Resistance to UV-induced cell-killing in nucleophosmin/B23 overexpressed NIH 3T3 fibroblasts: enhancement of DNA repair and up-regulation of PCNA in association with nucleophosmin/B23 overexpression. Carcinogenesis **23:**93–100.
42. **Yung, B. Y., A. M. Bor, and P. K. Chan.** 1990. Short exposure to actinomycin D induces "reversible" translocation of protein B23 as well as "reversible" inhibition of cell growth and RNA synthesis in HeLa cells. Cancer Res. **50:**5987–5991.
43. **Zambrowicz, B. P., G. A. Friedrich, E. C. Buxton, S. L. Lilleberg, C. Person, and A. T. Sands.** 1998. Disruption and sequence identification of 2,000 genes in mouse embryonic stem cells. Nature **392:**608–611.